Texas Coastal Nutrient Input Repository - Task 3 Report Lavaca Bay Water Quality Responses to Nutrient Loading

Texas Water Resources Institute TR-546
February 2023

Texas Water Resources Institute
make every drop count

Michael Schramm
Texas Water Resources Institute

Texas Coastal Nutrient Input Repository - Task 3 Report Lavaca Bay Water Quality Responses to Nutrient Loading

Michael Schramm [1]

[1] Research Specialist,
Texas Water Resources Institute, Texas A&M AgriLife Research
College Station, Texas

Texas Water Resources Institute Technical Report – 546
February 2023

Cover photo: Lavaca River by Michael Schramm

Table of Contents

Table of Figures

Table of Tables

Abbreviations

Acronym	Meaning
DO	Dissolved Oxygen
GAM	Generalized Additive Model
NO_x	Nitrite+Nitrate
NO_3-N	Nitrate-Nitrogen
QAPP	Quality Assurance Project Plan
SWQMIS	Surface Water Quality Monitoring Information System
TCEQ	Texas Commission on Environmental Quality
TKN	Total Kjeldahl Nitrogen
TP	Total Phosphorus
TWDB	Texas Water Development Board
USGS	United States Geological Survey

Summary

Links between freshwater inflows, watershed nutrient loads and water quality in Lavaca Bay were explored using generalized additive models. This approach allowed exploration of nonlinear relationships between upstream inputs and water quality responses while accounting for changes in water quality due to natural variations in precipitation and streamflow. Results show increasing concentrations of inorganic and organic nitrogen at select sites in Lavaca Bay, but no evidence of significant changes in chlorophyll-*a* or DO concentrations in recent years. Changes in freshwater inflow and, to a smaller extent, changes in watershed nutrient loading explain the variability in observed in total phosphorus and nitrite+nitrate concentrations. Limited data and complex responses of chlorophyll-*a*, Total Kjeldahl Nitrogen, and dissolved oxygen to freshwater inflow and nutrient loadings point to a need for continued data collection and model development. Overall, the study provides a baseline assessment of how management activities in the watershed that are aimed at reducing nonpoint source pollution are linked with water quality in Lavaca Bay to-date.

Introduction

Lavaca Bay is a secondary bay in the Matagorda Bay system located on the Texas Gulf coast, roughly halfway between the cities of Houston and Corpus Christi (Figure 1). Although Lavaca Bay faces substantial challenges associated with legacy contaminants, general water quality such as dissolved oxygen (DO), nutrients, and biological parameters indicates that ambient conditions in Lavaca Bay meet state water quality standards. The potential of degrading biological and physical conditions is an identified concern of local stakeholders. Significant long-term declines in benthic fauna abundance, biomass, and diversity in Lavaca Bay are linked to reductions in freshwater inflows and increases in estuary salinity (Beseres Pollack et al. 2011; Palmer and Montagna 2015; Montagna et al. 2020). More recently, Bugica et al. (2020) identified long-term monotonic increasing trends in Total Phosphorus (TP), Orthophosphate (PO_4^{-3}), Total Kjeldahl Nitrogen (TKN), and chlorophyll-*a* concentrations at sites within Lavaca Bay. Significant decreases in pH at all sites assessed by Bugica et al. (2020) in Lavaca Bay also point to long-term decreases in freshwater inflow and a resulting increase in salinity. Although no long-term changes in DO concentrations were identified, the trends in nutrient concentrations remain a concern. Nitrogen has been identified as a limiting factor for primary production in many Texas estuaries (Gardner et al. 2006; Hou et al. 2012; Dorado et al. 2015; Wetz et al. 2017; Paudel et al. 2019) and substantial changes in nitrogen loading could have ramifications for productivity and eutrophication in Lavaca Bay.

There are ongoing efforts between local entities and state and federal agencies to address water quality impairments and concerns in the freshwater portions of the Lavaca Bay watershed (Jain et al. 2018; Schramm et al. 2018; Berthold et al. 2021). On a statewide scale, these types of approaches have not resulted in desired successes and emphasizes a need to improve efforts at assessing and linking water quality improvements with management actions (Schramm et al. 2022). Therefore, there is a need to provide robust analysis of water quality responses where these efforts are taking place to identify approaches that are working or need improvement. Changes and trends in estuary water quality are non-linear and confounded by short and long-term changes in precipitation and runoff that hinder traditional data driven analytic methods (Wazniak et al. 2007; Lloyd et al. 2014). Water quality conditions should be evaluated relative to changes in environmental drivers such as precipitation and discharge to understand the effects of land use management and changes in nutrient loading on in-estuary water quality. This report presents methodology and results for assessing nonlinear linkages between selected water quality parameters in Lavaca Bay and freshwater inflows and nutrient loadings from the Lavaca Bay watershed.
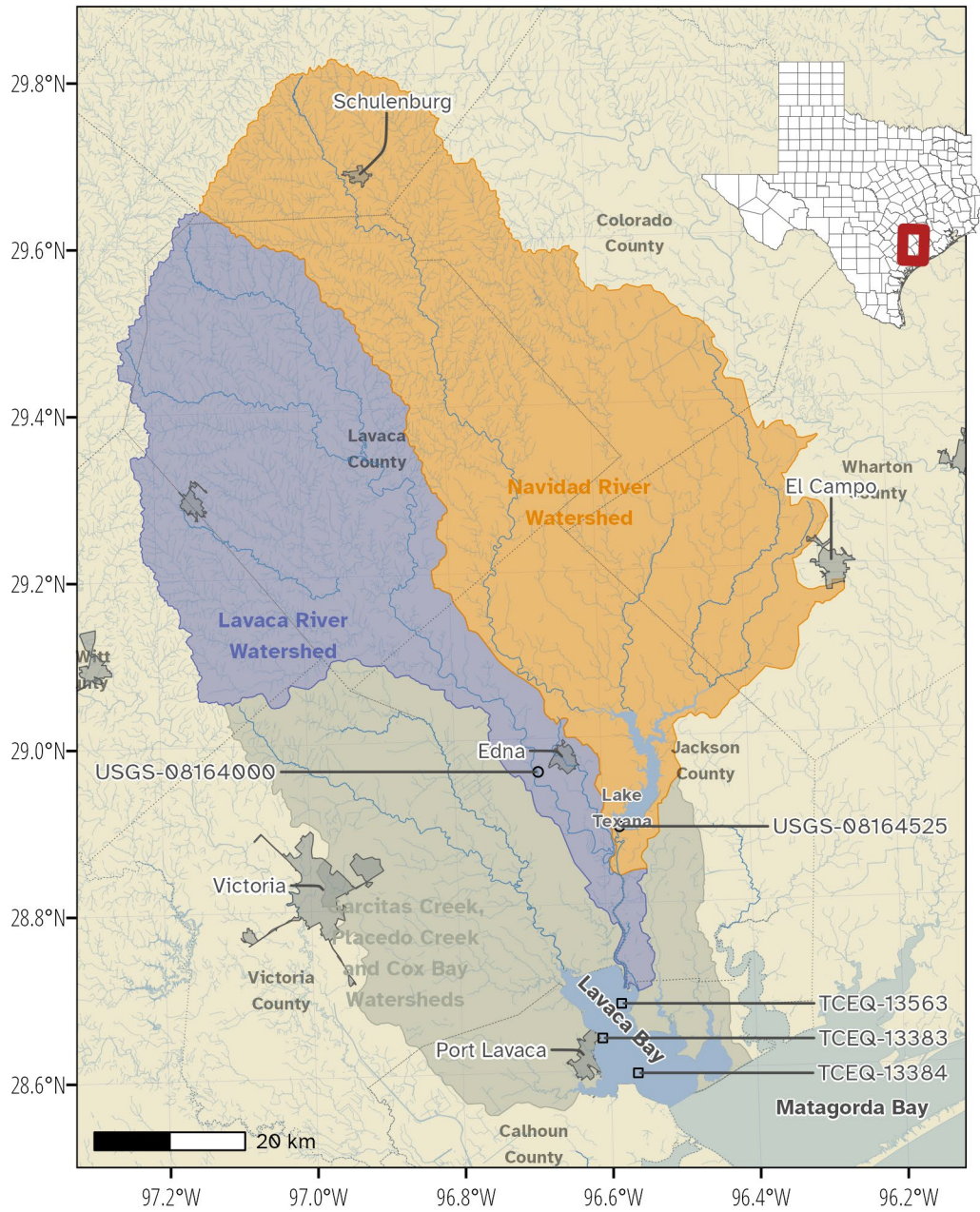
Figure 1. Study area map.

Methods

Study Area and Data

Lavaca Bay is 190 km^2 with the majority of freshwater inflow provided by the Lavaca-Navidad River system (Figure 1). The Garcitas-Arenosa, Placedo Creek, and Cox Bay watersheds provide additional freshwater inflows. The watershed land area for Lavaca Bay is 8,149 km^2. The Lavaca-Navidad River watershed is 5,966 km^2, or approximately 73% of the watershed area. Discharge from the Navidad River is regulated by Lake Texana which has been in operation since 1980. Lake Texana provides 170,000 acre-feet of water storage and discharges into the tidal section of the Navidad River, which ultimately joins the tidal section of the Lavaca River 15 km upstream of the confluence with the Bay.

Daily inflow to Lavaca Bay was estimated by combining mean daily discharge from USGS-08164000 (Lavaca River) and USGS-08164525 (Lake Texana). Mean daily discharges from USGS-08164000 were obtained from the United States Geologic Survey (USGS) National Water Information System using the *dataRetrieval* R package (De Cicco et al. 2022). Mean daily discharges for USGS-0816425 were obtained from the Texas Water Development Board (TWDB) (April 21, 2022, email from R. Neupane, TWDB). Daily nutrient loads were modeled at USGS-08164000 and USGS-08164525 using a Generalized Additive Model (GAM) relating time, season, and discharge to nutrient concentrations. The development of daily loads is described in Schramm (2023). Water quality data collected between January 2005 and December 2020 was obtained for three sites (TCEQ-13563, TCEQ-13383, TCEQ-13384) in Lavaca Bay from the Texas Commission on Environmental Quality's (TCEQ) Surface Water Quality Monitoring Information System (SWQMIS; https://www80.tceq.texas.gov/SwqmisWeb/public/crpweb.faces). Data housed in SWQMIS are collected under projects with an approved Quality Assurance Project Plan (QAPP) and under sample collection and lab methods procedures outlined by TCEQ's procedures manuals (https://www.tceq.texas.gov/waterquality/monitoring/swqm_guides.html). The QAPP and procedures manuals ensure consistent collection and analytical methods are applied between samples collected among different entities and different projects.

Table 1. Summary statistics of water quality parameters at Lavaca Bay sites.

Station ID	Station Description	Chlorophyll-*a* (µg/L)		Dissolved Oxygen (mg/L)		Nitrite+Nitrate (mg/L)		Total Kjeldahl Nitrogen (mg/L)		Total Phosphorus (mg/L)	
		Mean (SD)	N	Mean (SD)	N	Mean (SD)	N	Mean (SD)	N	Mean (SD)	N
TCEQ-13383	LAVACA BAY AT SH 35	9.43 (5.31)	47	7.22 (1.35)	55	0.07 (0.15)	51	0.94 (0.49)	45	0.11 (0.05)	47
TCEQ-13384	LAVACA BAY AT Y AT CM 66	8.22 (6.44)	46	7.51 (1.32)	54	0.06 (0.08)	52	0.76 (0.40)	48	0.08 (0.03)	51
TCEQ-13563	LAVACA BAY AT CM 22	9.67 (5.33)	49	7.91 (1.34)	56	0.09 (0.13)	53	0.94 (0.37)	49	0.13 (0.06)	50

Linking Watershed Loads to Estuary Water Quality

We explored relationships between freshwater inflow, watershed nutrient loads, and estuary water quality concentrations at each of the three monitoring sites in Lavaca Bay. The models used in this study were specified as GAM regression models. GAMs are a semiparametric version of generalized linear models where the linear predictor is represented as the sum of multiple unknown smooth functions and parametric linear predictors (Wood 2011). We fit GAMs using the *mgcv* package in R which makes available multiple types of smooth functions with automatic smoothness selection (Wood 2011). By using a GAM regression approach, the models used in this study can incorporate expected non-linear relationships, specify the exponential distribution family of the response, and specify a link function that relate the expected response to the predictors. The general forms of the three GAM models were:

$$g(\mu) = \alpha + f_1(ddate) + f_2(yday) \qquad (1)$$

$$g(\mu) = \alpha + f_1(ddate) + f_2(yday) + f_3(Q) \qquad (2)$$

$$g(\mu) = \alpha + f_1(ddate) + f_2(yday) + f_3(Q) + f_4(Load) \qquad (3)$$

where μ is the conditional expected response (nutrient concentration), $g()$ is the log link, α is the intercept, and $f_n()$ represents unknown smoothing functions. The response variable was modeled as Gamma distributed with mean μ and scale λ. $f_1(ddate)$ is decimal date smoothed with a thin-plate regression spline, $f_2(yday)$ is the numeric day of year smoothed with a cyclic cubic regression spline, $f_3(Q)$ is mean daily inflow (as measured at Lavaca River and Lake Texana), and $f_4(Load)$ is total NO_3-N or TP watershed load. Basis dimensions smooths were checked using the *gam.check* function to ensure models were not oversmoothed. Model residuals were inspected for distributional assumptions using the *gratia* package (Simpson 2022).

The relatively large impact of flow variability on nutrient loading creates a challenge for disentangling the impacts of inflow and load (Murphy et al. 2022). Instead of using raw freshwater inflow and nutrient loading values, these values were replaced by seasonally adjusted inflow and flow-adjusted nutrient loads as proposed by Murphy et al. (2022). To implement this approach, we fit a GAM relating season (day of the year) to log transformed daily inflow values:

$$g(\mu) = \alpha + f_1(yday) \qquad (4)$$

and a GAM relating log transformed NO$_3$-N or TP loads to log transformed daily streamflow:

$$g(\mu) = \alpha + f_1(Q) \qquad (5)$$

where the response variables were modeled as normally distributed with an identity link function. Response residuals from the respective GAM models were used as Q and *Load* in Equation (2) and Equation (3).

By comparing the model fits between the three GAMs, we evaluated if variances in Lavaca Bay water quality parameters are well explained by only temporal predictors, Equation (1), or if freshwater inflow, Equation (2), and nutrient loading, Equation (3), explain additional water quality parameter variation. To compare models, we used an information theoretic approach utilizing corrected Akaike information criterion (AIC$_c$) to calculate model probabilities as a measure of strength of evidence (Burnham et al. 2011).

A summary of models used for each parameter is shown in Table 2. Daily NO$_3$-N loading was used as a predictor for Nitrite+Nitrate (NO$_x$) concentrations, daily TP loading was used as a predictor for TP concentration, both NO$_3$-N and TP loads were used for DO and chlorophyll-*a* concentrations. TKN models were restricted to temporal and inflow terms because neither total nitrogen nor TKN loadings were available. Currently, insufficient data is available to estimate organic nitrogen loadings in the watershed but with ongoing monitoring projects incorporating a full suite of nutrient parameters, we anticipate the development of these loads in future years.

Table 2. Specification of GAM model structure.

Water Quality Response Parameter	Model	Model Structure
TP	Temporal	TP ~ s(ddate) + s(yday)
TP	Flow	TP ~ s(ddate) + s(yday) + s(Q)
TP	Flow+Load	TP ~ s(ddate) + s(yday) + s(Q) + s(TP Load)
NO_x	Temporal	NO_x ~ s(ddate) + s(yday)
NO_x	Flow	NO_x ~ s(ddate) + s(yday) + s(Q)
NO_x	Flow+Load	NO_x ~ s(ddate) + s(yday) + s(Q) + s(NO_3-N Load)
Chlorophyll-*a*	Temporal	Chlorophyll-*a* ~ s(ddate) + s(yday)
Chlorophyll-*a*	Flow	Chlorophyll-*a* ~ s(ddate) + s(yday) + s(Q)
Chlorophyll-*a*	Flow+Load	Chlorophyll-*a* ~ s(ddate) + s(yday) + s(Q) + s(TP Load) + s(NO_3-N Load)
Dissolved Oxygen	Temporal	DO ~ s(ddate) + s(yday)
Dissolved Oxygen	Flow	DO ~ s(ddate) + s(yday) + s(Q)
Dissolved Oxygen	Flow+Load	DO ~ s(ddate) + s(yday) + s(Q) + s(TP Load) + s(NO_3-N Load)
TKN	Temporal	TKN ~ s(ddate) + s(yday)
TKN	Flow	TKN ~ s(ddate) + s(yday) + s(Q)

Results

Temporal Trends

The long-term water quality concentration trends for each temporal GAM model are shown in Figure 2 and model summaries are included in Appendix A. No significant trends in TP were observed at any stations. Significant trends in NO_x concentrations were observed at TCEQ-13383 and TCEQ-13563. NO_x concentrations at TCEQ-13383 displayed a periodic pattern with changes in concentration generally following observed wet and dry period patterns in the watershed. In comparison, a linear increase in NO_x concentration was observed at TCEQ-13563. Significant trends in chlorophyll-*a* concentrations were observed at one site. The observed trend indicates a large decrease in chlorophyll-*a* from 2005-2015 with a more recent increase in concentration towards the long-term mean. Long-term trends in TKN were observed at one site. TCEQ-13383 shows a slight initial decrease in TKN below the mean concentration, followed by increases in TKN from 2010-2020. Although the other sites did not indicate statistical significance, the

predicted shape of the trends followed closely to TCEQ-13383. No significant trends in DO were observed between 2005 and 2020.
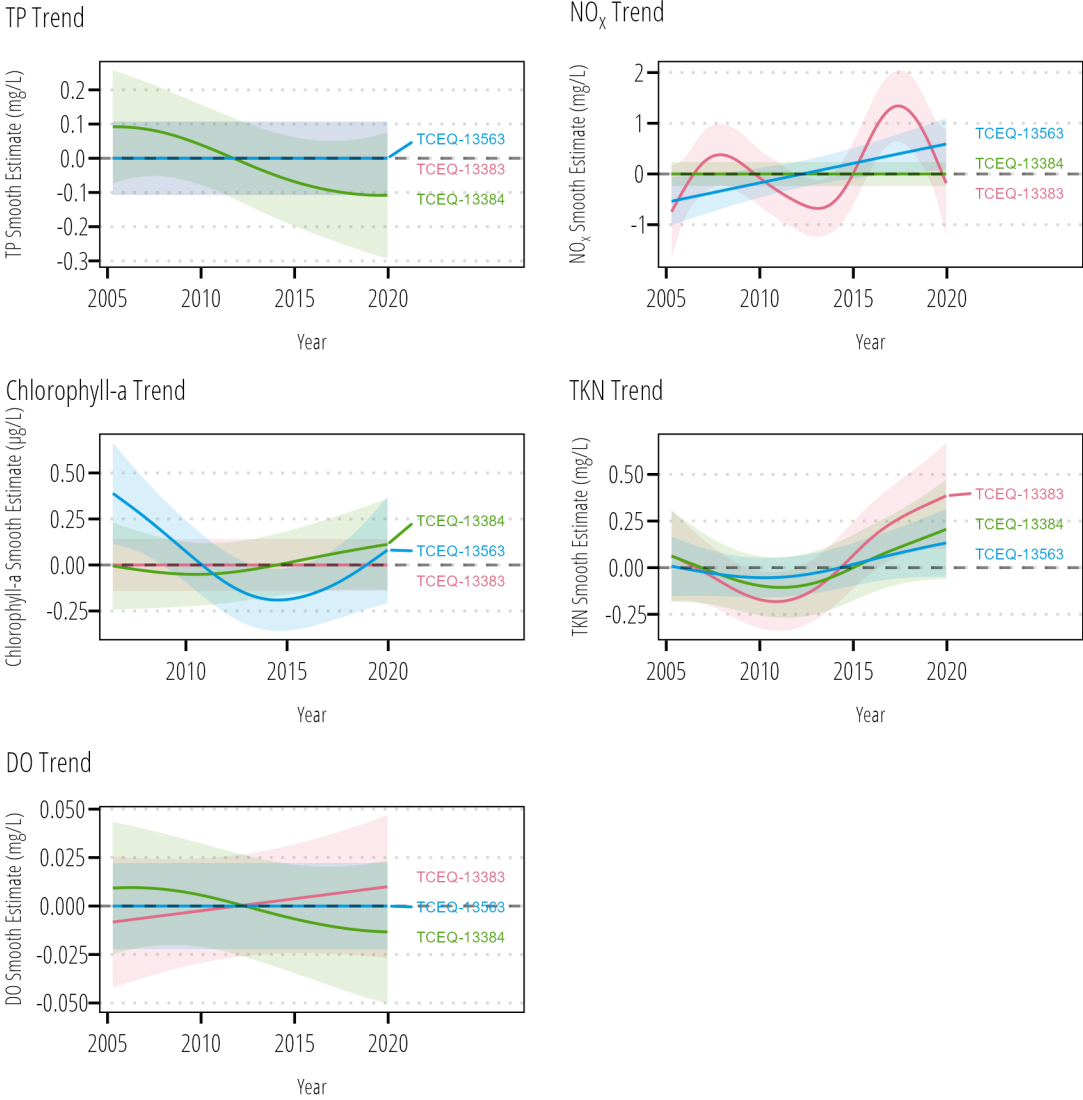
Figure 2. Smoothed long-term trend component from each water quality parameter and station GAM.

Estuarine Water Quality Explained by Freshwater Inflow and Load Variability

Inflow and/or nutrient load terms were significant for TP and NO$_x$ models at all three Lavaca Bay sites (Table 3). Chlorophyll-*a* models were improved by the inclusion of freshwater inflow at two sites. TKN and DO models were improved by the inclusion of freshwater inflow at one site. Inclusion of TP and NO$_3$-N loads did not improve Chlorophyll-*a* or DO models at any of the sites.

Table 3. Model AIC$_C$ values and associated model probabilities (in parenthesis). Models with the highest probability for each site and water quality parameter combination are bolded and italicized for emphasis.

Parameter	Site	Temporal	Flow	Flow + Load
TP	TCEQ-13383	-152.1 (0.03)	-156.1 (0.24)	***-158.2 (0.72)***
	TCEQ-13384	-194.4 (0.03)	***-200.2 (0.49)***	-200.2 (0.49)
	TCEQ-13563	-145.3 (0.00)	-156.6 (0.41)	***-157.3 (0.59)***
NO$_x$	TCEQ-13383	-218.9 (0.00)	***-244.8 (0.50)***	-244.8 (0.50)
	TCEQ-13384	-263.4 (0.00)	-311.7 (0.48)	***-311.9 (0.52)***
	TCEQ-13563	-175.1 (0.00)	***-190.2 (0.50)***	-190.2 (0.50)
Chlorophyll-*a*	TCEQ-13383	279.7 (0.18)	***278.1 (0.41)***	278.1 (0.41)
	TCEQ-13384	***268.2 (0.33)***	268.2 (0.33)	268.2 (0.33)
	TCEQ-13563	289.5 (0.08)	***286.1 (0.46)***	286.1 (0.46)
TKN	TCEQ-13383	***42.2 (0.66)***	43.5 (0.34)	NA
	TCEQ-13384	***34.3 (0.57)***	34.8 (0.43)	NA
	TCEQ-13563	31.1 (0.22)	***28.7 (0.78)***	NA
DO	TCEQ-13383	***146.4 (0.34)***	146.4 (0.34)	146.5 (0.32)
	TCEQ-13384	***135.9 (0.47)***	137.0 (0.27)	137.0 (0.27)
	TCEQ-13563	138.3 (0.25)	***137.2 (0.43)***	137.8 (0.32)

The estimated effects of freshwater inflow and nutrient loads are shown in Figure 3 and Figure 4. All three sites displayed a similar non-linear effect of adjusted inflow on TP and NO$_x$ concentration, with concentrations falling below the mean at lower flows and plateauing at higher inflow values.

A linear increase in chlorophyll-*a* was observed with freshwater inflow at TCEQ-13383. The increase in chlorophyll-*a* at TCEQ-13563 levels off and decreases at the highest inflow values. TCEQ-13563 was the only site where inflow had a significant effect on TKN concentration. The effect of streamflow on DO concentrations was only significant at TCEQ-13563 which displayed decreasing concentrations at both high and low inflows. The

effect size of inflow on DO concentration at TCEQ-13563 was relatively small (approximately 0.1 mg/L) and may not be biologically relevant even if statistically significant.
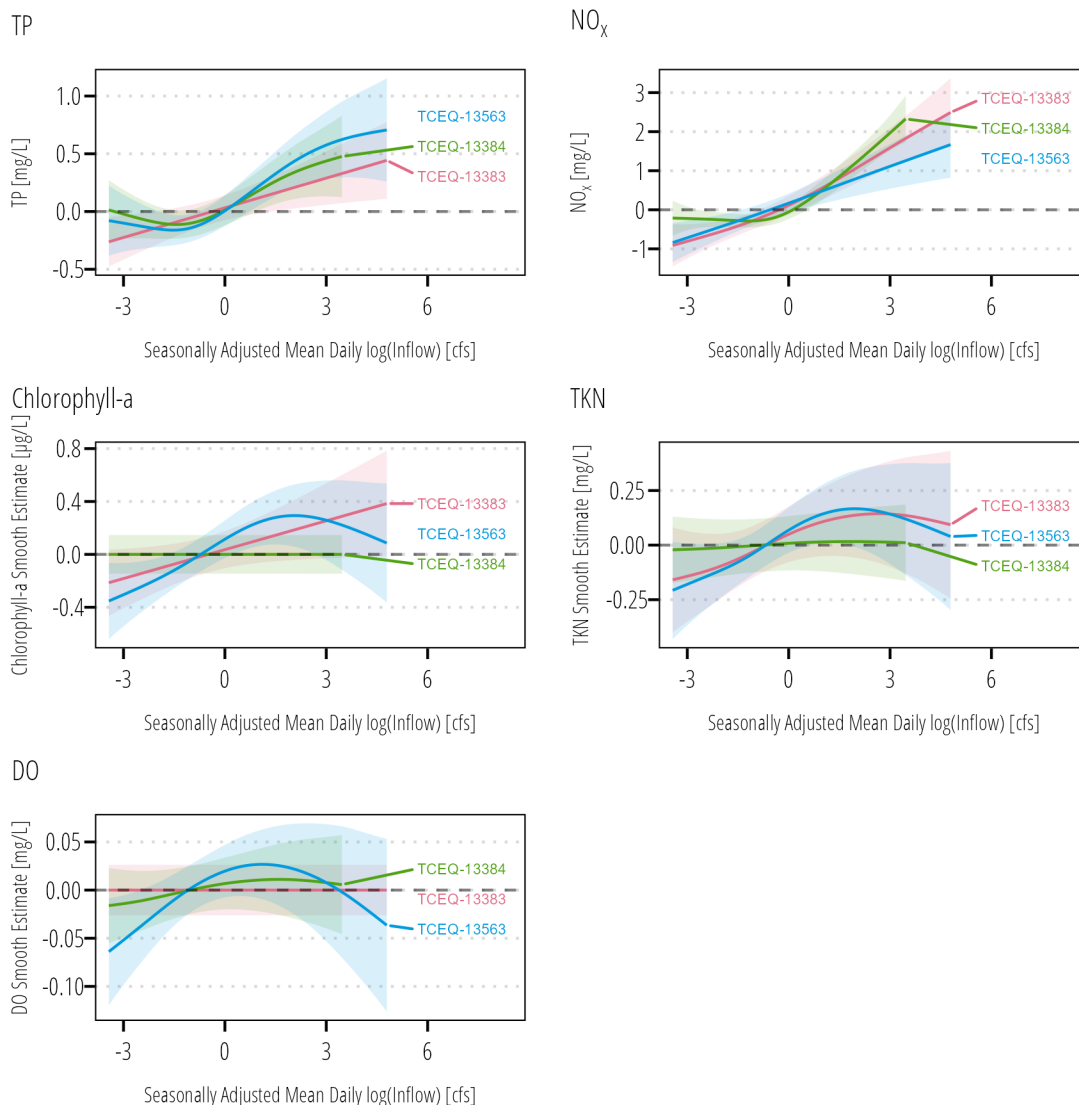
Figure 3. Estimated effects of seasonally adjusted mean daily inflow (response residuals from streamflow and season GAM model) on TP, NO_x, chlorophyll-a, TKN, and DO concentrations in Lavaca Bay.

Flow adjusted TP loads showed a positive linear effect on TP concentrations at TCEQ-13383 and TCEQ-13563 (Figure 3). Flow adjusted NO_3-N loads only had significant positive effects on concentration at TCEQ-13384. The relative effect sizes of nutrient loading were smaller than the effect of freshwater inflow at sites with significant effects (Table 3).
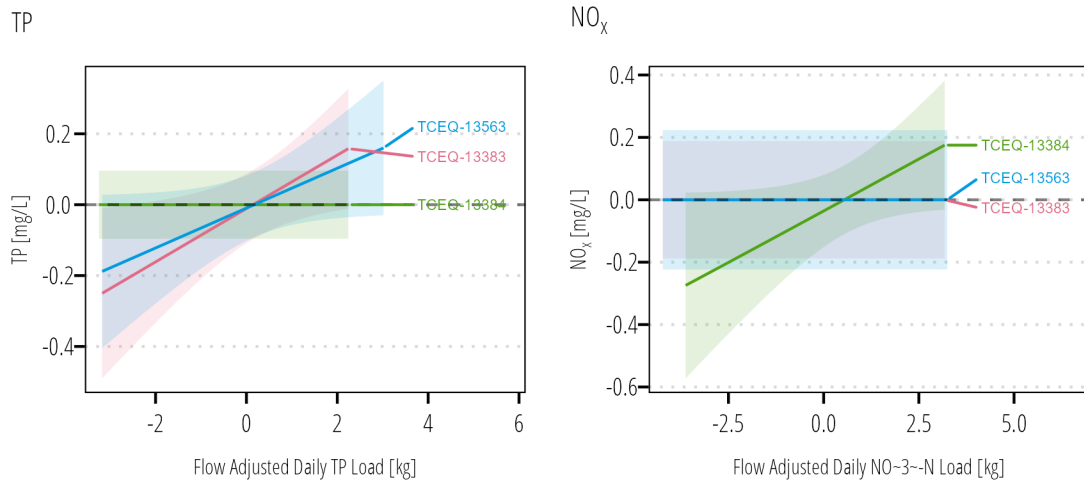
Figure 4. Estimated effects of flow adjusted nutrient loads (response residuals from nutrient load and flow GAM model) on TP and NO$_x$ concentrations in Lavaca Bay.

Discussion

The observed mix of non-linear water quality trends from 2005-2020 differs slightly from the trends identified by Bugica et al. (2020) for Lavaca Bay from 2009-2016, which is not unexpected considering the different time period and methodology. In comparison to estuaries on the Texas coast that are experiencing heavy development pressures, larger demands for freshwater diversions, increasing amounts of wastewater discharges, and more intense agricultural production (Wetz et al. 2016; Bugica et al. 2020), the long-term responses of DO and chlorophyll-a concentrations in Lavaca Bay appear generally stable. Due to low observed organic nitrogen and inorganic nitrogen concentrations in Lavaca Bay (Table 1) and nitrogen limitations observed in Texas coastal estuaries (Gardner et al. 2006; Hou et al. 2012; Dorado et al. 2015; Wetz et al. 2017; Paudel et al. 2019), the most concerning trends are the increasing concentrations of NO$_x$ at the upper Lavaca Bay TCEQ-13563 station and more recent increases in TKN concentrations at the mid-Bay TCEQ-13383 site.

The strong positive effect of freshwater inflow on NO$_x$, TKN, and TP are consistent with other studies relating runoff with nutrient concentrations in Lavaca Bay and other estuaries (Russell et al. 2006; Caffrey et al. 2007; Peierls et al. 2012; Palmer and Montagna 2015; Cira et al. 2021). The positive relationship between both NO$_x$ and TP with freshwater inflow suggests nonpoint watershed sources of inorganic nitrogen and TP at all three sites. Inflow has a non-linear relationship with TKN at the two upstream sites, with TKN increasing as freshwater inflow transitions from low to moderate levels. At higher freshwater inflows, the effect is attenuated, possibly indicating a flushing effect at higher

freshwater inflow. No relationship between TKN and freshwater inflow were observed at TCEQ-13384 located in the lower reach of Lavaca Bay. Tidal flushing from Matagorda Bay might be responsible for decreasing TKN concentrations and limiting the effects of freshwater inflow in lower reaches of Lavaca Bay. Russell et al. (2006) suggested the processing of organic loads in the upper portions of Lavaca Bay reduces the transport of nutrients into the lower reaches of the Bay.

Freshwater inflow has a strong positive effect on chlorophyll-*a* at the two stations closer to the mouth of the Lavaca River. The upper Bay site, TCEQ-13563, showed a decrease in chlorophyll-*a* concentrations at highest freshwater inflow volumes. These effects are observed in many riverine estuaries where nutrient limitations at low flows limit primary production and flushing effects or increasing turbidity reduce production at high flows (Peierls et al. 2012; Cloern et al. 2014). We did not observe a relationship between inorganic nitrogen or TP with chlorophyll-*a*. Due to the lack of TKN loading data, we are unable to ascertain potential relationships between chlorophyll-*a* and organic nitrogen loadings in Lavaca Bay. Although other studies have identified complex relationships between estuary nutrient concentrations, nutrient loading, and chlorophyll-*a* concentrations in Texas estuaries (Örnólfsdóttir et al. 2004; Dorado et al. 2015; Cira et al. 2021; Tominack and Wetz 2022), this study specifically used flow adjusted freshwater derived nutrient loads to parse out contributions from changes in nutrient loadings while accounting for variations in load due to flow. One explanation for the lack of observed significant effects of nutrient loading on various water quality parameters (nutrients, chlorophyll-*a* and DO) is the relatively small variation in flow-normalized loads within the Lavaca River watershed. The time-period in this study is relatively short and recent, any variation in flow-adjusted nutrient concentrations would rely on changes in must be attributed to non-point source changes or changes in nutrient retention at Lake Texana. Water quality management in the watershed has focused largely on voluntary adoption of agricultural best management practices (Schramm et al. 2018; Berthold et al. 2021). The challenges with adoption of practices and scaling field/site water quality improvements to watershed level water quality improvements are well documented (Sharpley et al. 2009; Meals et al. 2010; Liu et al. 2018). As a result, the relative reductions of non-point sources of nutrients are arguably more challenging to achieve and may result in smaller reductions relative to reductions achieved through point source reductions. In other watersheds with longer periods of data, the largest reductions in nutrients have been attributed to point-source reductions associated with elimination of phosphorus contents in detergents and upgrades to wastewater facilities in the 1980s (Paerl et al. 2006; Harding et al. 2016), which resulted in large load reductions regardless of natural variation in streamflows. In comparison, the temporal changes of flow normalized TP loads in this study were not significant at either of the downstream freshwater sites in the watershed (Schramm,

2023). Significant increases in flow-normalized NO_3-N loads were observed in the Lavaca River from 2008 through 2009, followed by significant decreases after 2017. These variations in NO_3-N loads from the Lavaca River may be masked, especially during wet periods, by the discharges from Lake Texana which accounts for approximately 74% of watershed NO_3-N loads annually.

For all the sites, season explained most of the variation in DO concentrations (see DO GAM Model Summaries in Appendix A). Freshwater inflow and nutrient loadings did not have a significant effect on DO concentrations. Responses of estuary metabolic processes and resulting DO concentrations can be quite complicated and often locally specific (Caffrey 2004). While the lack of total nitrogen or TKN loading data hinders interpretation, the large seasonal effect on DO suggests physical factors play an important role and should be included in future models. Russell suggested that Lavaca Bay may not be limited by nutrients alone, with high turbidity or processing of organic loads in upper portions of the Bay limiting production. Additionally, inflows and nutrient loads from point and nonpoint sources along the bay, and the Placedo and Garcitas Creeks watershed, may be important influences on metabolic responses that hinder the ability to detect signals in the GAM models.

Study Limitations

The clearest limitation of this study is the lack of data informing organic nitrogen loading into Lavaca Bay. Monitoring programs in the freshwater sections of the watershed are now including Total Nitrogen and TKN in their laboratory analysis under TCEQ procedures. To date, less than five years of data is available and several more years of routine data (and preferably flow-biased sampling) is needed to develop reliable estimates of TKN and Total Nitrogen loadings. Future efforts will look to build these datasets and assessments.

Estuary water quality assessments following storms and large discharge events show that flow disturbances can have lagged effects lasting days to as long as months (Mooney and McClelland 2012; Wetz and Yoskowitz 2013; Bukaveckas et al. 2020; Walker et al. 2021). The approach used in this study only accounts for same daydischarges and nutrient loads and do not account for pulses of nutrient or freshwater that may have occurred in prior days that are likely to have long lasting water quality impacts. Extending the GAM analysis with antecedent discharge terms such as flow anomalies (Vecchia et al. 2009) or exponentially discounted flow (Kuhnert et al. 2012) and associated antecedent load terms could provide additional insight into the lagged effects associated with freshwater inflows and nutrient loads on estuary water quality.

This study utilized separate GAM models to describe relationships between response variables and potential covariates at each site. A formal comparison of models between sites is not appropriate because the models assume independence between observations. A logical next step to this work is to assess how water quality responses change across sites. A spatiotemporal GAM model (see Liu et al. (2020) for an example) across that Bay would incorporate all observations and model concentration as a function of space (latitude and longitude) and time. However, this approach would provide limited information with only three water quality sites in Lavaca Bay and would require substantially more data to identify significant effects. Hierarchical GAMs provide an approach to incorporate observations from all sites within a model while allowing smoothers to vary by site. This approach provides a statistically valid approach for assessing how relationships between water quality and covariates vary between sites and across sites (Pedersen et al. 2019). Although we do not expect substantial differences in identified effects, the Hierarchical GAM is a natural follow-up to this study to better describe differences between sites. This would be of particular value in similar estuary studies where changes in watershed nutrient loading are expected to result in a response in estuary water quality.

Conclusion

Consistent with other studies along the Texas coast, this study provides evidence that variation in freshwater inflow has a strong effect on nutrient and chlorophyll-*a* concentrations. However, we did not find strong effects of freshwater flow on DO concentrations, which were dominated by seasonal variation. Inference about the effect of flow-adjusted nutrient loading on estuary water quality was limited by the relatively small observed variance in flow-adjusted nutrient loads from the Lavaca River watershed. Increases in TP loading had small linear effects on TP concentration at the upper and middle Lavaca Bay sites and no effect at the lower site. Increases in NO_3-N loads did not have a significant effect at any of the Lavaca Bay sites. We also failed to find strong evidence for direct effects of flow-adjusted NO_3-N and TP loading with chlorophyll-*a* and DO concentrations. Although we did not identify strong effects from flow-adjusted nutrient loading, the results are valuable for providing a baseline assessment of how management activities in the watershed that are aimed at reducing nonpoint source pollutants are linked with water quality in Lavaca Bay to-date.

The complex nature of estuary metabolic and hydrologic processes suggests the relationship between nutrient loading and estuary water quality is not direct. To continue assessing the linkages between upstream management activities and estuary water

quality, more comprehensive models can be developed but will require increased efforts in data collection and analysis. Some of these efforts are already underway or being pursued and will provide valuable information for local stakeholders and resource managers.

Bibliography

Berthold TA, Olsovsky T, Schramm MP. 2021. Direct mailing education campaign impacts on the adoption of grazing management practices. Journal of Contemporary Water Research & Education. (174):45–60. doi:10.1111/j.1936-704X.2021.3360.x.

Beseres Pollack J, Palmer T, Montagna P. 2011. Long-term trends in the response of benthic macrofauna to climate variability in the Lavaca-Colorado Estuary, Texas. Mar Ecol Prog Ser. 436:67–80. doi:10.3354/meps09267.

Bugica K, Sterba-Boatwright B, Wetz MS. 2020. Water quality trends in Texas estuaries. Marine Pollution Bulletin. 152:110903. doi:10.1016/j.marpolbul.2020.110903.

Bukaveckas PA, Tassone S, Lee W, Franklin RB. 2020. The influence of storm events on metabolism and water quality of riverine and estuarine segments of the James, Mattaponi, and Pamunkey Rivers. Estuaries and Coasts. 43(7):1585–1602. doi:10.1007/s12237-020-00819-9.

Burnham KP, Anderson DR, Huyvaert KP. 2011. AIC model selection and multimodel inference in behavioral ecology: some background, observations, and comparisons. Behav Ecol Sociobiol. 65(1):23–35. doi:10.1007/s00265-010-1029-6.

Caffrey JM. 2004. Factors controlling net ecosystem metabolism in U.S. estuaries. Estuaries. 27(1):90–101. doi:10.1007/BF02803563.

Caffrey JM, Chapin TP, Jannasch HW, Haskins JC. 2007. High nutrient pulses, tidal mixing and biological response in a small California estuary: Variability in nutrient concentrations from decadal to hourly time scales. Estuarine, Coastal and Shelf Science. 71(3-4):368–380. doi:10.1016/j.ecss.2006.08.015.

Cira EK, Palmer TA, Wetz MS. 2021. Phytoplankton dynamics in a low-inflow estuary (Baffin Bay, TX) during drought and high-rainfall conditions associated with an El Niño event. Estuaries and Coasts. 44(7):1752–1764. doi:10.1007/s12237-021-00904-7.

Cloern JE, Foster SQ, Kleckner AE. 2014. Phytoplankton primary production in the world's estuarine-coastal ecosystems. Biogeosciences. 11(9):2477–2501. doi:10.5194/bg-11-2477-2014.

De Cicco LA, Hirsch RM, Lorenz DL, Watkins WD, Johnson M. 2022. dataRetrieval: R packages for discovering and retrieving water data available from Federal hydrologic web services. doi:10.5066/P9X4L3GE. https://code.usgs.gov/water/dataRetrieval.

Dorado S, Booe T, Steichen J, McInnes AS, Windham R, Shepard A, Lucchese AEB, Preischel H, Pinckney JL, Davis SE, et al. 2015. Towards an understanding of the interactions between freshwater inflows and phytoplankton communities in a subtropical estuary in the Gulf of Mexico. PLoS ONE. 10(7):e0130931. doi:10.1371/journal.pone.0130931.

Gardner WS, McCarthy MJ, An S, Sobolev D, Sell KS, Brock D. 2006. Nitrogen fixation and dissimilatory nitrate reduction to ammonium (DNRA) support nitrogen dynamics in Texas estuaries. Limnol Oceanogr. 51(1part2):558–568. doi:10.4319/lo.2006.51.1_part_2.0558.

Harding LW, Gallegos CL, Perry ES, Miller WD, Adolf JE, Mallonee ME, Paerl HW. 2016. Long-term trends of nutrients and phytoplankton in Chesapeake Bay. Estuaries and Coasts. 39(3):664–681. doi:10.1007/s12237-015-0023-7.

Hou L, Liu M, Carini SA, Gardner WS. 2012. Transformation and fate of nitrate near the sediment–water interface of Copano Bay. Continental Shelf Research. 35:86–94. doi:10.1016/j.csr.2012.01.004.

Jain S, Ruff S, Schramm MP. 2018. Technical Support Document for One Total Maximum Daily Load for Indicator Bacteria in Arenosa Creek. Austin, TX: Texas Commission on Environmental Quality Report No.: AS-203. https://www.tceq.texas.gov/downloads/water-quality/tmdl/arenosa-creek-recreational-108/108-arenosa-creek-tsd-final-10-02-20.pdf.

Kuhnert PM, Henderson BL, Lewis SE, Bainbridge ZT, Wilkinson SN, Brodie JE. 2012. Quantifying total suspended sediment export from the Burdekin River catchment using the loads regression estimator tool. Water Resour Res. 48(4). doi:10.1029/2011WR011080.

Liu L, Dong Y, Kong M, Zhou J, Zhao H, Wang Y, Zhang M, Wang Z. 2020. Towards the comprehensive water quality control in Lake Taihu: Correlating chlorophyll a and water quality parameters with generalized additive model. Science of The Total Environment. 705:135993. doi:10.1016/j.scitotenv.2019.135993.

Liu T, Bruins R, Heberling M. 2018. Factors influencing farmers' adoption of best management practices: A review and synthesis. Sustainability. 10(2):432. doi:10.3390/su10020432.

Lloyd CEM, Freer JE, Collins AL, Johnes PJ, Jones JI. 2014. Methods for detecting change in hydrochemical time series in response to targeted pollutant mitigation in river catchments. Journal of Hydrology. 514:297–312. doi:10.1016/j.jhydrol.2014.04.036.

Meals DW, Dressing SA, Davenport TE. 2010. Lag time in water quality response to best management practices: A review. Journal of Environment Quality. 39(1):85. doi:10.2134/jeq2009.0108.

Montagna PA, Cockett PM, Kurr EM, Trungale J. 2020. Assessment of the Relationship Between Freshwater Inflow and Biological Indicators in Lavaca Bay. Corpus Christi, Texas: Harte Research Institute, Texas A&M University-Corpus Christi Final Report to the Texas Water Development Board Report No.: Contract # 1800012268.

Mooney RF, McClelland JW. 2012. Watershed export events and ecosystem responses in the Mission–Aransas National Estuarine Research Reserve, South Texas. Estuaries and Coasts. 35(6):1468–1485. doi:10.1007/s12237-012-9537-4.

Murphy RR, Keisman J, Harcum J, Karrh RR, Lane M, Perry ES, Zhang Q. 2022. Nutrient improvements in Chesapeake Bay: Direct effect of load reductions and implications for coastal management. Environ Sci Technol. 56(1):260–270. doi:10.1021/acs.est.1c05388.

Örnólfsdóttir EB, Lumsden SE, Pinckney JL. 2004. Nutrient pulsing as a regulator of phytoplankton abundance and community composition in Galveston Bay, Texas. Journal of Experimental Marine Biology and Ecology. 303(2):197–220. doi:10.1016/j.jembe.2003.11.016.

Paerl HW, Valdes LM, Piehler MF, Stow CA. 2006. Assessing the effects of nutrient management in an estuary experiencing climatic change: The Neuse River Estuary, North Carolina. Environmental Management. 37(3):422–436. doi:10.1007/s00267-004-0034-9.

Palmer TA, Montagna PA. 2015. Impacts of droughts and low flows on estuarine water quality and benthic fauna. Hydrobiologia. 753(1):111–129. doi:10.1007/s10750-015-2200-x.

Paudel B, Montagna PA, Adams L. 2019. The relationship between suspended solids and nutrients with variable hydrologic flow regimes. Regional Studies in Marine Science. 29:100657. doi:10.1016/j.rsma.2019.100657.

Pedersen EJ, Miller DL, Simpson GL, Ross N. 2019. Hierarchical generalized additive models in ecology: an introduction with mgcv. PeerJ. 7:e6876. doi:10.7717/peerj.6876.

Peierls BL, Hall NS, Paerl HW. 2012. Non-monotonic responses of phytoplankton biomass accumulation to hydrologic variability: A comparison of two coastal plain North Carolina Estuaries. Estuaries and Coasts. 35(6):1376–1392. doi:10.1007/s12237-012-9547-2.

Russell MJ, Montagna PA, Kalke RD. 2006. The effect of freshwater inflow on net ecosystem metabolism in Lavaca Bay, Texas. Estuarine, Coastal and Shelf Science. 68(1-2):231–244. doi:10.1016/j.ecss.2006.02.005.

Schramm MP, Berthold A, Entwistle C, Peddicord K. 2018. Lavaca River Watershed Protection Plan. College Station, Texas: Texas Water Resources Institute Report No.: TR-507. https://twri.tamu.edu/media/1456/tr-507.pdf.

Schramm MP, Gitter A, Gregory L. 2022. Total Maximum Daily Loads and *Escherichia coli* trends in Texas freshwater streams. Journal of Contemporary Water Research & Education.(176):36–49. doi:10.1111/j.1936-704X.2022.3374.x.

Schramm M. 2023. Texas Coastal Nutrient Input Repository - Task 4 Report Statistical Models for Nutrient Loading into Lavaca Bay. College Station, TX: Texas Water Resources Institute Report No.: TR-543. https://twri.tamu.edu/media/6170/tr_543.pdf.

Sharpley AN, Kleinman PJA, Jordan P, Bergström L, Allen AL. 2009. Evaluating the success of phosphorus management from field to watershed. Journal of Environment Quality. 38(5):1981. doi:10.2134/jeq2008.0056.

Simpson GL. 2022. gratia: Graceful Graceful ggplot-Based Graphics and Other Functions for GAMs Fitted using mgcv. https://gavinsimpson.github.io/gratia/.

Tominack SA, Wetz MS. 2022. Variability in phytoplankton biomass and community composition in Corpus Christi Bay, Texas. Estuaries and Coasts. doi:10.1007/s12237-022-01137-y.

Vecchia AV, Gilliom RJ, Sullivan DJ, Lorenz DL, Martin JD. 2009. Trends in concentrations and use of agricultural herbicides for Corn Belt Rivers, 1996–2006. Environ Sci Technol. 43(24):9096–9102. doi:10.1021/es902122j.

Walker LM, Montagna PA, Hu X, Wetz MS. 2021. Timescales and magnitude of water quality change in three Texas estuaries induced by passage of Hurricane Harvey. Estuaries and Coasts. 44(4):960–971. doi:10.1007/s12237-020-00846-6.

Wazniak CE, Hall MR, Carruthers TJB, Sturgis B, Dennison WC, Orth RJ. 2007. Linking water quality to living resources in a Mid-Atlantic lagoon system, USA. Ecological Applications. 17(sp5):S64–S78. doi:10.1890/05-1554.1.

Wetz MS, Cira EK, Sterba-Boatwright B, Montagna PA, Palmer TA, Hayes KC. 2017. Exceptionally high organic nitrogen concentrations in a semi-arid South Texas estuary susceptible to brown tide blooms. Estuarine, Coastal and Shelf Science. 188:27–37. doi:10.1016/j.ecss.2017.02.001.

Wetz MS, Hayes KC, Fisher KVB, Price L, Sterba-Boatwright B. 2016. Water quality dynamics in an urbanizing subtropical estuary (Oso Bay, Texas). Marine Pollution Bulletin. 104(1-2):44–53. doi:10.1016/j.marpolbul.2016.02.013.

Wetz MS, Yoskowitz DW. 2013. An "extreme" future for estuaries? Effects of extreme climatic events on estuarine water quality and ecology. Marine Pollution Bulletin. 69(1-2):7–18. doi:10.1016/j.marpolbul.2013.01.020.

Wood SN. 2011. Fast stable restricted maximum likelihood and marginal likelihood estimation of semiparametric generalized linear models: Estimation of Semiparametric Generalized Linear Models. Journal of the Royal Statistical Society: Series B (Statistical Methodology). 73(1):3–36. doi:10.1111/j.1467-9868.2010.00749.x.

Appendix A - GAM Model Summaries

Total Phosphorus GAM Model Summaries

TCEQ-13563

Table 4. Temporal GAM summary for TP concentration at TCEQ-13563.

Component	Term	Estimate	Std Error	t-value	p-value	
A. parametric coefficients	(Intercept)	-2.052	0.065	-31.636	0.0000	***

Component	Term	edf	Ref. df	F-value	p-value	
B. smooth terms	s(day)	1.419	3.000	1.327	0.0642	.
	s(ddate)	0.000	19.000	0.000	0.5354	

Signif. codes: 0 <= '***' < 0.001 < '**' < 0.01 < '*' < 0.05

Adjusted R-squared: 0.071, Deviance explained 0.104

-REML : -73.311, Scale est: 0.210, N: 50

Table 5. Inflow GAM summary for TP concentration at TCEQ-13563.

Component	Term	Estimate	Std Error	t-value	p-value	
A. parametric coefficients	(Intercept)	-2.078	0.058	-35.901	0.0000	***

Component	Term	edf	Ref. df	F-value	p-value	
B. smooth terms	s(inflow)	2.186	7.000	2.184	0.0008	***
	s(day)	0.638	3.000	0.266	0.2885	
	s(ddate)	0.000	19.000	0.000	0.9722	

Signif. codes: 0 <= '***' < 0.001 < '**' < 0.01 < '*' < 0.05

Adjusted R-squared: 0.344, Deviance explained 0.347

-REML : -78.843, Scale est: 0.167, N: 50

Table 6. Inflow plus load GAM summary for TP concentration at TCEQ-13563.

Component	Term	Estimate	Std Error	t-value	p-value	
A. parametric coefficients	(Intercept)	-2.084	0.056	-37.418	0.0000	***

Component	Term	edf	Ref. df	F-value	p-value	
B. smooth terms	s(inflow)	2.183	7.000	2.074	0.0010	**
	s(TP load)	0.738	7.000	0.357	0.0665	.
	s(day)	1.130	3.000	0.707	0.1512	
	s(ddate)	0.000	19.000	0.000	0.9511	

Signif. codes: 0 <= '***' < 0.001 < '**' < 0.01 < '*' < 0.05

Adjusted R-squared: 0.378, Deviance explained 0.407

-REML : -79.480, Scale est: 0.155, N: 50

Table 7. Temporal GAM summary for TP concentration at TCEQ-13383.

Component	Term	Estimate	Std Error	t-value	p-value	
A. parametric coefficients	(Intercept)	-2.252	0.066	-34.284	0.0000	***

Component	Term	edf	Ref. df	F-value	p-value	
B. smooth terms	s(day)	1.835	3.000	3.349	0.0052	**
	s(ddate)	0.000	19.000	0.000	0.7181	

Signif. codes: 0 <= '***' < 0.001 < '**' < 0.01 < '*' < 0.05

Adjusted R-squared: 0.163, Deviance explained 0.209

-REML : -76.343, Scale est: 0.203, N: 47

Table 8. Inflow GAM summary for TP concentration at TCEQ-13383.

Component	Term	Estimate	Std Error	t-value	p-value	
A. parametric coefficients	(Intercept)	-2.264	0.063	-35.666	0.0000	***

Component	Term	edf	Ref. df	F-value	p-value	
B. smooth terms	s(inflow)	0.846	7.000	0.765	0.0146	*
	s(day)	1.662	3.000	2.213	0.0204	*
	s(ddate)	0.000	19.000	0.000	0.9560	

Signif. codes: 0 <= '***' < 0.001 < '**' < 0.01 < '*' < 0.05

Adjusted R-squared: 0.257, Deviance explained 0.302

-REML : -78.284, Scale est: 0.189, N: 47

Table 9. Inflow plus load GAM summary for TP concentration at TCEQ-13383.

Component	Term	Estimate	Std Error	t-value	p-value	
A. parametric coefficients	(Intercept)	-2.273	0.059	-38.421	0.0000	***

Component	Term	edf	Ref. df	F-value	p-value	
B. smooth terms	s(inflow)	0.843	7.000	0.791	0.0130	*
	s(TP load)	0.771	7.000	0.504	0.0350	*
	s(day)	1.840	3.000	3.291	0.0054	**
	s(ddate)	0.000	19.000	0.000	0.8997	

Signif. codes: 0 <= '***' < 0.001 < '**' < 0.01 < '*' < 0.05

Adjusted R-squared: 0.334, Deviance explained 0.372

-REML : -79.145, Scale est: 0.164, N: 47

Table 10. Temporal GAM summary for TP concentration at TCEQ-13384.

Component	Term	Estimate	Std Error	t-value	p-value	
A. parametric coefficients	(Intercept)	-2.563	0.061	-42.167	0.0000	***

Component	Term	edf	Ref. df	F-value	p-value	
B. smooth terms	s(day)	0.634	3.000	0.345	0.2011	
	s(ddate)	0.895	19.000	0.129	0.0739	.

Signif. codes: 0 <= '***' < 0.001 < '**' < 0.01 < '*' < 0.05

Adjusted R-squared: 0.0664, Deviance explained 0.0839

-REML : -98.633, Scale est: 0.188, N: 51

Table 11. Inflow GAM summary for TP concentration at TCEQ-13384.

Component	Term	Estimate	Std Error	t-value	p-value	
A. parametric coefficients	(Intercept)	-2.577	0.058	-44.244	0.0000	***

Component	Term	edf	Ref. df	F-value	p-value	
B. smooth terms	s(inflow)	1.772	7.000	1.130	0.0121	*
	s(day)	0.000	3.000	0.000	0.3897	
	s(ddate)	0.814	19.000	0.256	0.0180	*

Signif. codes: 0 <= '***' < 0.001 < '**' < 0.01 < '*' < 0.05

Adjusted R-squared: 0.192, Deviance explained 0.210

-REML : -100.336, Scale est: 0.173, N: 51

Table 12. Inflow plus load GAM summary for TP concentration at TCEQ-13384.

Component	Term	Estimate	Std Error	t-value	p-value	
A. parametric coefficients	(Intercept)	-2.577	0.058	-44.244	0.0000	***

Component	Term	edf	Ref. df	F-value	p-value	
B. smooth terms	s(inflow)	1.772	7.000	1.130	0.0121	*
	s(TP load)	0.000	7.000	0.000	0.3461	
	s(day)	0.000	3.000	0.000	0.3897	
	s(ddate)	0.814	19.000	0.256	0.0180	*

Signif. codes: 0 <= '***' < 0.001 < '**' < 0.01 < '*' < 0.05

Adjusted R-squared: 0.192, Deviance explained 0.210

-REML : -100.336, Scale est: 0.173, N: 51

Nitrite+Nitrate GAM Model Summaries

TCEQ-13563

Table 13. Temporal GAM summary for NO$_x$ concentration at TCEQ-13563.

Component	Term	Estimate	Std Error	t-value	p-value	
A. parametric coefficients	(Intercept)	-2.772	0.156	-17.805	0.0000	***

Component	Term	edf	Ref. df	F-value	p-value	
B. smooth terms	s(day)	2.400	4.000	3.617	0.0014	**
	s(ddate)	0.911	8.000	0.637	0.0200	*

Signif. codes: 0 <= '***' < 0.001 < '**' < 0.01 < '*' < 0.05

Adjusted R-squared: 0.155, Deviance explained 0.352

-REML : -87.865, Scale est: 1.284, N: 53

Table 14. Inflow GAM summary for NO$_x$ concentration at TCEQ-13563.

Component	Term	Estimate	Std Error	t-value	p-value	
A. parametric coefficients	(Intercept)	-2.901	0.136	-21.388	0.0000	***

Component	Term	edf	Ref. df	F-value	p-value	
B. smooth terms	s(inflow)	1.034	6.000	2.036	0.0007	***
	s(day)	2.458	4.000	3.125	0.0036	**
	s(ddate)	0.724	8.000	0.208	0.1330	

Signif. codes: 0 <= '***' < 0.001 < '**' < 0.01 < '*' < 0.05

Adjusted R-squared: 0.459, Deviance explained 0.527

-REML : -95.240, Scale est: 0.975, N: 53

Table 15. Inflow plus load GAM summary for NO_x concentration at TCEQ-13563.

Component	Term	Estimate	Std Error	t-value	p-value	
A. parametric coefficients	(Intercept)	-2.901	0.136	-21.388	0.0000	

Component	Term	edf	Ref. df	F-value	p-value	
B. smooth terms	s(inflow)	1.034	6.000	2.036	0.0007	
	s(NO_3-N load)	0.000	7.000	0.000	0.4168	
	s(day)	2.458	4.000	3.125	0.0036	**
	s(ddate)	0.724	8.000	0.208	0.1330	

Signif. codes: 0 <= '***' < 0.001 < '**' < 0.01 < '*' < 0.05

Adjusted R-squared: 0.459, Deviance explained 0.527

-REML : -95.240, Scale est: 0.975, N: 53

Table 16. Temporal GAM summary for NO$_x$ concentration at TCEQ-13383.

Component	Term	Estimate	Std Error	t-value	p-value	
A. parametric coefficients	(Intercept)	-3.314	0.154	-21.459	0.0000	***

Component	Term	edf	Ref. df	F-value	p-value	
B. smooth terms	s(day)	1.878	4.000	0.972	0.1172	
	s(ddate)	5.328	8.000	2.028	0.0122	*

Signif. codes: 0 <= '***' < 0.001 < '**' < 0.01 < '*' < 0.05

Adjusted R-squared: 0.130, Deviance explained 0.594

-REML : -104.729, Scale est: 1.216, N: 51

Table 17. Inflow GAM summary for NO$_x$ concentration at TCEQ-13383.

Component	Term	Estimate	Std Error	t-value	p-value	
A. parametric coefficients	(Intercept)	-3.395	0.114	-29.685	0.0000	***

Component	Term	edf	Ref. df	F-value	p-value	
B. smooth terms	s(inflow)	1.700	6.000	5.631	0.0000	***
	s(day)	2.103	4.000	1.627	0.0359	*
	s(ddate)	0.535	8.000	0.092	0.2407	

Signif. codes: 0 <= '***' < 0.001 < '**' < 0.01 < '*' < 0.05

Adjusted R-squared: 0.356, Deviance explained 0.706

-REML : -122.152, Scale est: 0.667, N: 51

Table 18. Inflow plus load GAM summary for NO$_x$ concentration at TCEQ-13383.

Component	Term	Estimate	Std Error	t-value	p-value
A. parametric coefficients	(Intercept)	-3.395	0.114	-29.685	0.0000

Component	Term	edf	Ref. df	F-value	p-value
B. smooth terms	s(inflow)	1.700	6.000	5.631	0.0000
	s(NO$_3$-N load)	0.000	7.000	0.000	0.7255
	s(day)	2.103	4.000	1.627	0.0359
	s(ddate)	0.535	8.000	0.092	0.2407

Signif. codes: 0 <= '***' < 0.001 < '**' < 0.01 < '*' < 0.05

Adjusted R-squared: 0.356, Deviance explained 0.706

-REML : -122.152, Scale est: 0.667, N: 51

Table 19. Temporal GAM summary for NO$_x$ concentration at TCEQ-13384.

Component	Term	Estimate	Std Error	t-value	p-value	
A. parametric coefficients	(Intercept)	-3.515	0.143	-24.641	0.0000	***

Component	Term	edf	Ref. df	F-value	p-value	
B. smooth terms	s(day)	3.476	4.000	4.258	0.0024	**
	s(ddate)	0.000	8.000	0.000	0.6599	

Signif. codes: 0 <= '***' < 0.001 < '**' < 0.01 < '*' < 0.05

Adjusted R-squared: 0.0626, Deviance explained 0.494

-REML : -129.606, Scale est: 1.058, N: 52

Table 20. Inflow GAM summary for NO$_x$ concentration at TCEQ-13384.

Component	Term	Estimate	Std Error	t-value	p-value	
A. parametric coefficients	(Intercept)	-3.667	0.069	-53.529	0.0000	***

Component	Term	edf	Ref. df	F-value	p-value	
B. smooth terms	s(inflow)	2.947	6.000	10.531	0.0000	***
	s(day)	2.113	4.000	2.318	0.0085	**
	s(ddate)	0.001	8.000	0.000	0.4346	

Signif. codes: 0 <= '***' < 0.001 < '**' < 0.01 < '*' < 0.05

Adjusted R-squared: 0.650, Deviance explained 0.813

-REML : -152.911, Scale est: 0.244, N: 52

Table 21. Inflow plot load GAM summary for NO_x concentration at TCEQ-13384.

Component	Term	Estimate	Std Error	t-value	p-value	
A. parametric coefficients	(Intercept)	-3.673	0.066	-55.273	0.0000	

Component	Term	edf	Ref. df	F-value	p-value	
B. smooth terms	s(inflow)	3.024	6.000	10.621	0.0000	
	s(NO_3-N load)	0.791	7.000	0.395	0.0613	.
	s(day)	2.013	4.000	1.948	0.0152	
	s(ddate)	0.000	8.000	0.000	0.5535	

Signif. codes: 0 <= '***' < 0.001 < '**' < 0.01 < '*' < 0.05

Adjusted R-squared: 0.664, Deviance explained 0.826

-REML : -153.724, Scale est: 0.230, N: 52

Chlorophyll-*a* GAM Model Summaries

TCEQ-13563

Table 22. Temporal GAM summary for chlorophyll-*a* concentration at TCEQ-13563

Component	Term	Estimate	Std Error	t-value	p-value	
A. parametric coefficients	(Intercept)	2.223	0.070	31.640	0.0000	***

Component	Term	edf	Ref. df	F-value	p-value	
B. smooth terms	s(day)	1.540	3.000	1.874	0.0292	*
	s(ddate)	1.857	19.000	0.421	0.0135	*

Signif. codes: 0 <= '***' < 0.001 < '**' < 0.01 < '*' < 0.05

Adjusted R-squared: 0.191, Deviance explained 0.274

-REML : 143.945, Scale est: 0.242, N: 49

Table 23. Inflow GAM summary for chlorophyll-*a* concentration at TCEQ-13563

Component	Term	Estimate	Std Error	t-value	p-value	
A. parametric coefficients	(Intercept)	2.204	0.064	34.186	0.0000	***

Component	Term	edf	Ref. df	F-value	p-value	
B. smooth terms	s(inflow)	1.721	7.000	1.153	0.0092	**
	s(day)	1.413	3.000	1.401	0.0534	.
	s(ddate)	1.867	19.000	0.573	0.0032	**

Signif. codes: 0 <= '***' < 0.001 < '**' < 0.01 < '*' < 0.05

Adjusted R-squared: 0.336, Deviance explained 0.401

-REML : 141.519, Scale est: 0.204, N: 49

Table 24. Inflow plus load GAM summary for chlorophyll-*a* concentration at TCEQ-13563

Component	Term	Estimate	Std Error	t-value	p-value	
A. parametric coefficients	(Intercept)	2.204	0.064	34.186	0.0000	

Component	Term	edf	Ref. df	F-value	p-value	
B. smooth terms	s(inflow)	1.721	7.000	1.153	0.0092	**
	s(NO$_3$-N load)	0.000	7.000	0.000	0.6622	
	s(TP load)	0.000	7.000	0.000	0.9689	
	s(day)	1.413	3.000	1.401	0.0534	.
	s(ddate)	1.867	19.000	0.573	0.0032	**

Signif. codes: 0 <= '***' < 0.001 < '**' < 0.01 < '*' < 0.05

Adjusted R-squared: 0.336, Deviance explained 0.401

-REML : 141.519, Scale est: 0.204, N: 49

Table 25. Temporal GAM summary for chlorophyll-*a* concentration at TCEQ-13383

Component	Term	Estimate	Std Error	t-value	p-value	
A. parametric coefficients	(Intercept)	2.221	0.086	25.913	0.0000	***

Component	Term	edf	Ref. df	F-value	p-value	
B. smooth terms	s(day)	1.463	3.000	1.362	0.0662	.
	s(ddate)	0.000	19.000	0.000	0.4683	

Signif. codes: 0 <= '***' < 0.001 < '**' < 0.01 < '*' < 0.05

Adjusted R-squared: 0.0856, Deviance explained 0.121

-REML : 139.015, Scale est: 0.345, N: 47

Table 26. Inflow GAM summary for chlorophyll-*a* concentration at TCEQ-13383

Component	Term	Estimate	Std Error	t-value	p-value	
A. parametric coefficients	(Intercept)	2.211	0.082	26.819	0.0000	***

Component	Term	edf	Ref. df	F-value	p-value	
B. smooth terms	s(inflow)	0.777	7.000	0.405	0.0602	.
	s(day)	1.274	3.000	0.914	0.1211	
	s(ddate)	0.000	19.000	0.000	0.5367	

Signif. codes: 0 <= '***' < 0.001 < '**' < 0.01 < '*' < 0.05

Adjusted R-squared: 0.153, Deviance explained 0.183

-REML : 138.076, Scale est: 0.320, N: 47

Table 27. Inflow plus load GAM summary for chlorophyll-*a* concentration at TCEQ-13383

Component	Term	Estimate	Std Error	t-value	p-value
A. parametric coefficients	(Intercept)	2.211	0.082	26.819	0.0000

Component	Term	edf	Ref. df	F-value	p-value	
B. smooth terms	s(inflow)	0.777	7.000	0.405	0.0602	.
	s(NO$_3$-N load)	0.000	7.000	0.000	0.6871	
	s(TP load)	0.000	7.000	0.000	0.8833	
	s(day)	1.274	3.000	0.914	0.1211	
	s(ddate)	0.000	19.000	0.000	0.5371	

Signif. codes: 0 <= '***' < 0.001 < '**' < 0.01 < '*' < 0.05

Adjusted R-squared: 0.153, Deviance explained 0.183

-REML : 138.076, Scale est: 0.320, N: 47

Table 28. Temporal GAM summary for chlorophyll-*a* concentration at TCEQ-13384

Component	Term	Estimate	Std Error	t-value	p-value	
A. parametric coefficients	(Intercept)	2.032	0.088	22.968	0.0000	***

Component	Term	edf	Ref. df	F-value	p-value	
B. smooth terms	s(day)	2.583	3.000	4.373	0.0047	**
	s(ddate)	0.701	19.000	0.053	0.2400	

Signif. codes: 0 <= '***' < 0.001 < '**' < 0.01 < '*' < 0.05

Adjusted R-squared: 0.155, Deviance explained 0.285

-REML : 134.757, Scale est: 0.360, N: 46

Table 29. Inflow GAM summary for chlorophyll-*a* concentration at TCEQ-13384

Component	Term	Estimate	Std Error	t-value	p-value	
A. parametric coefficients	(Intercept)	2.032	0.088	22.967	0.0000	***

Component	Term	edf	Ref. df	F-value	p-value	
B. smooth terms	s(inflow)	0.000	7.000	0.000	0.7248	
	s(day)	2.583	3.000	4.372	0.0047	**
	s(ddate)	0.700	19.000	0.052	0.2401	

Signif. codes: 0 <= '***' < 0.001 < '**' < 0.01 < '*' < 0.05

Adjusted R-squared: 0.155, Deviance explained 0.285

-REML : 134.757, Scale est: 0.360, N: 46

Table 30. Inflow plus load GAM summary for chlorophyll-*a* concentration at TCEQ-13384

Component	Term	Estimate	Std Error	t-value	p-value	
A. parametric coefficients	(Intercept)	2.032	0.088	22.967	0.0000	

Component	Term	edf	Ref. df	F-value	p-value	
B. smooth terms	s(inflow)	0.000	7.000	0.000	0.7091	
	s(NO$_3$-N load)	0.000	7.000	0.000	0.7937	
	s(TP load)	0.000	7.000	0.000	0.7602	
	s(day)	2.583	3.000	4.372	0.0047	**
	s(ddate)	0.700	19.000	0.052	0.2401	

Signif. codes: 0 <= '***' < 0.001 < '**' < 0.01 < '*' < 0.05

Adjusted R-squared: 0.155, Deviance explained 0.285

-REML : 134.757, Scale est: 0.360, N: 46

TKN GAM Model Summaries

TCEQ-13563

Table 31. Temporal GAM summary for TKN concentraton at TCEQ-13563.

Component	Term	Estimate	Std Error	t-value	p-value
A. parametric coefficients	(Intercept)	-0.072	0.051	-1.416	0.1637

Component	Term	edf	Ref. df	F-value	p-value
B. smooth terms	s(day)	1.391	3.000	0.932	0.1367
	s(ddate)	1.201	19.000	0.113	0.1684

Signif. codes: 0 <= '***' < 0.001 < '**' < 0.01 < '*' < 0.05

Adjusted R-squared: 0.0824, Deviance explained 0.149

-REML : 14.523, Scale est: 0.128, N: 49

Table 32. Inflow GAM summary for TKN concentration at TCEQ-13563.

Component	Term	Estimate	Std Error	t-value	p-value	
A. parametric coefficients	(Intercept)	-0.075	0.050	-1.520	0.1356	

Component	Term	edf	Ref. df	F-value	p-value	
B. smooth terms	s(inflow)	1.608	7.000	0.740	0.0398	*
	s(day)	1.060	3.000	0.556	0.2108	
	s(ddate)	0.000	19.000	0.000	0.5366	

Signif. codes: 0 <= '***' < 0.001 < '**' < 0.01 < '*' < 0.05

Adjusted R-squared: 0.125, Deviance explained 0.196

-REML : 13.279, Scale est: 0.121, N: 49

Table 33. Temporal GAM summary for TKN concentration at TCEQ-13383.

Component	Term	Estimate	Std Error	t-value	p-value	
A. parametric coefficients	(Intercept)	-0.085	0.063	-1.346	0.1856	

Component	Term	edf	Ref. df	F-value	p-value	
B. smooth terms	s(day)	0.000	3.000	0.000	0.5278	
	s(ddate)	2.203	19.000	0.491	0.0122	*

Signif. codes: 0 <= '***' < 0.001 < '**' < 0.01 < '*' < 0.05

Adjusted R-squared: 0.124, Deviance explained 0.223

-REML : 21.204, Scale est: 0.181, N: 45

Table 34. Inflow GAM summary for TKN concentration at TCEQ-13383.

Component	Term	Estimate	Std Error	t-value	p-value	
A. parametric coefficients	(Intercept)	-0.088	0.064	-1.374	0.1769	

Component	Term	edf	Ref. df	F-value	p-value	
B. smooth terms	s(inflow)	1.125	7.000	0.352	0.1150	
	s(day)	0.000	3.000	0.000	0.6250	
	s(ddate)	1.814	19.000	0.273	0.0544	.

Signif. codes: 0 <= '***' < 0.001 < '**' < 0.01 < '*' < 0.05

Adjusted R-squared: 0.154, Deviance explained 0.254

-REML : 20.749, Scale est: 0.187, N: 45

Table 35. Temporal GAM summary for TKN concentration at TCEQ-13384.

Component	Term	Estimate	Std Error	t-value	p-value	
A. parametric coefficients	(Intercept)	-0.287	0.073	-3.945	0.0003	***

Component	Term	edf	Ref. df	F-value	p-value
B. smooth terms	s(day)	0.000	3.000	0.000	0.7689
	s(ddate)	1.524	19.000	0.154	0.1485

Signif. codes: 0 <= '***' < 0.001 < '**' < 0.01 < '*' < 0.05

Adjusted R-squared: 0.0426, Deviance explained 0.0938

-REML : 16.590, Scale est: 0.255, N: 48

Table 36. Inflow GAM summary for TKN concentration at TCEQ-13384.

Component	Term	Estimate	Std Error	t-value	p-value	
A. parametric coefficients	(Intercept)	-0.288	0.073	-3.962	0.0003	***

Component	Term	edf	Ref. df	F-value	p-value
B. smooth terms	s(inflow)	0.200	7.000	0.027	0.3811
	s(day)	0.000	3.000	0.000	0.7675
	s(ddate)	1.497	19.000	0.148	0.1542

Signif. codes: 0 <= '***' < 0.001 < '**' < 0.01 < '*' < 0.05

Adjusted R-squared: 0.0436, Deviance explained 0.0997

-REML : 16.583, Scale est: 0.254, N: 48

Dissolved Oxygen GAM Model Summaries

TCEQ-13563

Table 37. Temporal GAM summary for DO concentration at TCEQ-13563

Component	Term	Estimate	Std Error	t-value	p-value	
A. parametric coefficients	(Intercept)	2.060	0.014	152.339	0.0000	***

Component	Term	edf	Ref. df	F-value	p-value	
B. smooth terms	s(day)	2.663	3.000	29.706	0.0000	***
	s(ddate)	0.000	19.000	0.000	0.5000	

Signif. codes: 0 <= '***' < 0.001 < '**' < 0.01 < '*' < 0.05

Adjusted R-squared: 0.598, Deviance explained 0.647

-REML : 72.924, Scale est: 0.0102, N: 56

Table 38. Inflow GAM summary for DO concentration at TCEQ-13563

Component	Term	Estimate	Std Error	t-value	p-value	
A. parametric coefficients	(Intercept)	2.059	0.013	158.861	0.0000	***

Component	Term	edf	Ref. df	F-value	p-value	
B. smooth terms	s(inflow)	1.533	7.000	0.647	0.0522	.
	s(day)	2.692	3.000	31.795	0.0000	***
	s(ddate)	0.000	19.000	0.000	0.8661	

Signif. codes: 0 <= '***' < 0.001 < '**' < 0.01 < '*' < 0.05

Adjusted R-squared: 0.629, Deviance explained 0.686

-REML : 72.045, Scale est: 0.00941, N: 56

Table 39. Inflow plus load GAM summary for DO concentration at TCEQ-13563

Component	Term	Estimate	Std Error	t-value	p-value
A. parametric coefficients	(Intercept)	2.059	0.012	164.825	0.0000

Component	Term	edf	Ref. df	F-value	p-value
B. smooth terms	s(inflow)	1.762	7.000	1.012	0.0159
	s(NO$_3$-N load)	0.000	7.000	0.000	0.3201
	s(TP load)	1.419	7.000	0.412	0.1262
	s(day)	2.695	3.000	33.467	0.0000
	s(ddate)	0.000	19.000	0.000	0.8755

Signif. codes: 0 <= '***' < 0.001 < '**' < 0.01 < '*' < 0.05

Adjusted R-squared: 0.648, Deviance explained 0.716

-REML : 71.850, Scale est: 0.00874, N: 56

Table 40. Temporal GAM summary for DO concentration at TCEQ-13383

Component	Term	Estimate	Std Error	t-value	p-value	
A. parametric coefficients	(Intercept)	1.966	0.016	123.304	0.0000	***

Component	Term	edf	Ref. df	F-value	p-value	
B. smooth terms	s(day)	2.493	3.000	24.979	0.0000	***
	s(ddate)	0.285	19.000	0.021	0.2411	

Signif. codes: 0 <= '***' < 0.001 < '**' < 0.01 < '*' < 0.05

Adjusted R-squared: 0.547, Deviance explained 0.600

-REML : 75.725, Scale est: 0.014, N: 55

Table 41. Inflow GAM summary for DO concentration at TCEQ-13383

Component	Term	Estimate	Std Error	t-value	p-value	
A. parametric coefficients	(Intercept)	1.966	0.016	123.304	0.0000	***

Component	Term	edf	Ref. df	F-value	p-value	
B. smooth terms	s(inflow)	0.000	7.000	0.000	0.8622	
	s(day)	2.493	3.000	24.979	0.0000	***
	s(ddate)	0.285	19.000	0.021	0.2410	

Signif. codes: 0 <= '***' < 0.001 < '**' < 0.01 < '*' < 0.05

Adjusted R-squared: 0.547, Deviance explained 0.600

-REML : 75.725, Scale est: 0.014, N: 55

Table 42. Inflow plus load GAM summary for DO concentration at TCEQ-13383

Component	Term	Estimate	Std Error	t-value	p-value
A. parametric coefficients	(Intercept)	1.966	0.016	125.358	0.0000

Component	Term	edf	Ref. df	F-value	p-value
B. smooth terms	s(inflow)	0.000	7.000	0.000	0.8008
	s(NO$_3$-N load)	0.859	7.000	0.274	0.1102
	s(TP load)	0.000	7.000	0.000	0.8822
	s(day)	2.504	3.000	26.573	0.0000
	s(ddate)	0.106	19.000	0.006	0.2889

Signif. codes: 0 <= '***' < 0.001 < '**' < 0.01 < '*' < 0.05

Adjusted R-squared: 0.560, Deviance explained 0.618

-REML : 75.399, Scale est: 0.0135, N: 55

Table 43. Temporal GAM summary for DO concentration at TCEQ-13384

Component	Term	Estimate	Std Error	t-value	p-value	
A. parametric coefficients	(Intercept)	2.007	0.015	138.110	0.0000	***

Component	Term	edf	Ref. df	F-value	p-value	
B. smooth terms	s(day)	2.591	3.000	30.673	0.0000	***
	s(ddate)	0.535	19.000	0.044	0.2107	

Signif. codes: 0 <= '***' < 0.001 < '**' < 0.01 < '*' < 0.05

Adjusted R-squared: 0.611, Deviance explained 0.658

-REML : 70.737, Scale est: 0.0114, N: 54

Table 44. Inflow GAM summary for DO concentration at TCEQ-13384

Component	Term	Estimate	Std Error	t-value	p-value	
A. parametric coefficients	(Intercept)	2.006	0.014	140.003	0.0000	***

Component	Term	edf	Ref. df	F-value	p-value	
B. smooth terms	s(inflow)	0.558	7.000	0.119	0.2206	
	s(day)	2.592	3.000	31.377	0.0000	***
	s(ddate)	0.652	19.000	0.061	0.1725	

Signif. codes: 0 <= '***' < 0.001 < '**' < 0.01 < '*' < 0.05

Adjusted R-squared: 0.621, Deviance explained 0.669

-REML : 70.662, Scale est: 0.0111, N: 54

Table 45. Inflow plus load GAM summary for DO concentration at TCEQ-13384

Component	Term	Estimate	Std Error	t-value	p-value
A. parametric coefficients	(Intercept)	2.006	0.014	140.003	0.0000

Component	Term	edf	Ref. df	F-value	p-value
B. smooth terms	s(inflow)	0.558	7.000	0.118	0.2206
	s(NO$_3$-N load)	0.000	7.000	0.000	0.5777
	s(TP load)	0.000	7.000	0.000	0.3485
	s(day)	2.592	3.000	31.376	0.0000
	s(ddate)	0.652	19.000	0.061	0.1726

Signif. codes: 0 <= '***' < 0.001 < '**' < 0.01 < '*' < 0.05

Adjusted R-squared: 0.621, Deviance explained 0.669

-REML : 70.662, Scale est: 0.0111, N: 54